SMARCE1 is required for the invasive progression of in situ cancers

Ethan S. Sokol[a,b,1], Yu-Xiong Feng[a,1], Dexter X. Jin[a,b,1], Minu D. Tizabi[a], Daniel H. Miller[a,b], Malkiel A. Cohen[a], Sandhya Sanduja[a], Ferenc Reinhardt[a], Jai Pandey[a], Daphne A. Superville[a,b], Rudolf Jaenisch[a,b,2], and Piyush B. Gupta[a,b,c,d,2]

[a]Whitehead Institute for Biomedical Research, Cambridge, MA 02142; [b]Department of Biology, Massachusetts Institute of Technology, Cambridge, MA 02139; [c]Koch Institute for Integrative Cancer Research at MIT, Cambridge, MA 02139; and [d]Harvard Stem Cell Institute, Cambridge, MA 02138

Contributed by Rudolf Jaenisch, March 9, 2017 (sent for review November 30, 2016; reviewed by Philip W. Hinds and Victoria L. Seewaldt)

Advances in mammography have sparked an exponential increase in the detection of early-stage breast lesions, most commonly ductal carcinoma in situ (DCIS). More than 50% of DCIS lesions are benign and will remain indolent, never progressing to invasive cancers. However, the factors that promote DCIS invasion remain poorly understood. Here, we show that SMARCE1 is required for the invasive progression of DCIS and other early-stage tumors. We show that SMARCE1 drives invasion by regulating the expression of secreted proteases that degrade basement membrane, an ECM barrier surrounding all epithelial tissues. In functional studies, SMARCE1 promotes invasion of in situ cancers growing within primary human mammary tissues and is also required for metastasis in vivo. Mechanistically, SMARCE1 drives invasion by forming a SWI/SNF-independent complex with the transcription factor ILF3. In patients diagnosed with early-stage cancers, SMARCE1 expression is a strong predictor of eventual relapse and metastasis. Collectively, these findings establish SMARCE1 as a key driver of invasive progression in early-stage tumors.

DCIS | invasive progression | biomarker | SMARCE1

The past two decades have brought an exponential increase in the diagnosis of early-stage breast lesions, most commonly ductal carcinoma in situ (DCIS). DCIS remains encapsulated within the ductal-lobular architecture of mammary epithelium; in contrast, invasive breast cancers have escaped this architecture by breaking through the basement membrane, a layer of ECM rich in collagen (IV) and laminins that separates epithelial tissues from the adjacent stromal microenvironment (Fig. S1*A*) (1). This distinction has a critical impact on patient prognosis: whereas women with DCIS show no reduction in survival 5 y after diagnosis, those with invasive cancers have a 15–74% reduction in 5-y survival rates depending on the extent of tumor invasion at diagnosis (2).

Given these observations, there is significant interest in finding genes that promote the invasive progression of early-stage tumors (3). Previous studies have sought molecular alterations present in invasive tumors but not DCIS, leading to the identification of hundreds of genomic and gene-expression alterations specifically associated with invasive cancers (4–6). However, it is unclear if genes that are amplified or up-regulated in invasive cancers also functionally drive DCIS invasion. In large part, the difficulty in addressing this question can be traced to a paucity of experimental systems that model cancer invasion within a microenvironment that faithfully replicates human breast tissue.

The treatment of early-stage cancers remains an unresolved issue. Women with early-stage breast cancers—which include DCIS and stage I tumors that have not entered the lymph nodes—are typically treated by lumpectomy followed by localized radiation. However, recurrence with metastasis occurs in a significant fraction of women with stage I cancers; if such tumors could be prospectively identified, it would be possible to preemptively adopt a more aggressive therapy. Conversely, even though the standard treatment is curative for DCIS, more than half of these lesions are indolent and would never become life-threatening if left untreated (7–9), indicating that there is systematic overtreatment of a significant fraction of patients with DCIS. Collectively, these considerations underscore the importance of defining the genetic drivers of DCIS progression.

In the present study, we identify SMARCE1 as a key driver of early-stage tumor invasion and show that its expression in patients is a strong predictor of whether early-stage tumors will ultimately progress and metastasize.

Results

SMARCE1 Regulates an ECM Invasion Module That Is Up-Regulated upon DCIS Progression. Expression profiling studies have identified ∼350 genes that are up-regulated as DCIS tumors progress to invasive cancers (4). We hypothesized that upstream regulators of these transcriptional changes might be master regulators of DCIS progression. Genes with shared upstream regulators form "transcriptional modules" that exhibit correlated fluctuations in their expression (10). We identified two transcriptional modules associated with DCIS progression, containing genes that were highly correlated in their expression across 158 breast cancers (average $\rho = 0.44$, $P < 10^{-15}$; Fig. 1*A*, Fig. S1*B*, and *SI Materials and Methods*).

Significance

More than half of ductal carcinoma in situ (DCIS) lesions will never progress to invasive breast cancers. However, the factors that drive invasion are not well understood. Our findings establish SMARCE1 as a clinically relevant factor that promotes the invasive progression of early-stage breast cancers. SMARCE1 drives invasion by serving as a master regulator of genes encoding proinvasive ECM and proteases required to degrade basement membrane. In functional studies in 3D cultures and animal models, SMARCE1 is dispensable for tumor growth but is required for the invasive and metastatic progression of cancers. In patients, SMARCE1 expression specifically identifies early-stage breast, lung, and ovarian cancers that are likely to eventually progress and metastasize.

Author contributions: E.S.S., Y.-X.F., D.X.J., and P.B.G. designed research; E.S.S., Y.-X.F., D.X.J., M.D.T., D.H.M., F.R., and D.A.S. performed research; M.D.T. and M.A.C. performed microinjection experiments; D.H.M. and D.A.S. performed 3-D culture experiments; S.S. performed IHC experiments; F.R. performed animal experiments; R.J. provided essential guidance and reagents for the microinjection experiments; M.A.C. and R.J. contributed new reagents/analytic tools; E.S.S., Y.-X.F., D.X.J., S.S., and J.P. analyzed data; P.B.G. supervised the study; and P.B.G. wrote the paper.

Reviewers: P.W.H., Tufts Medical Center; and V.L.S., City of Hope.

The authors declare no conflict of interest.

Freely available online through the PNAS open access option.

Data deposition: The data reported in this paper have been deposited in the Gene Expression Omnibus (GEO) database (accession no. GSE96933).

[1]E.S.S., Y.-X.F., and D.X.J. contributed equally to this work.

[2]To whom correspondence may be addressed. Email: jaenisch@wi.mit.edu or piyush@mit.edu.

This article contains supporting information online at www.pnas.org/lookup/suppl/doi:10.1073/pnas.1703931114/-/DCSupplemental.

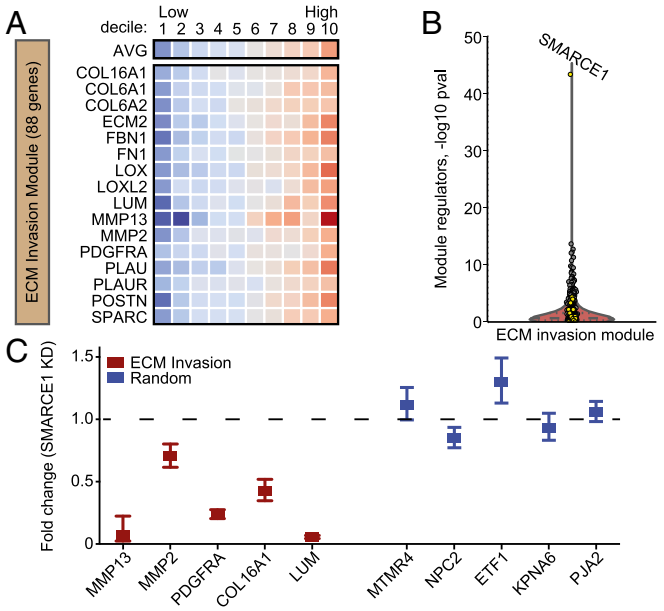

Fig. 1. SMARCE1 regulates an ECM invasion module that is up-regulated upon DCIS progression. (*A*) Expression of genes in the ECM invasion module across 158 primary human breast tumors. Tumors were sorted based on their average expression of the 88 genes in the module (AVG), and divided into ten groups (deciles). Heat map denotes the average expression in the corresponding decile. (*B*) Violin plot showing the contributions of 1,124 transcription and chromatin-modifying factors to expression of the ECM invasion module. Statistical significance was computed with the hypergeometric test. SWI/SNF complex genes are highlighted in yellow. (*C*) Quantitative PCR analysis of expression of ECM invasion module genes and random module genes in SUM159 cells transduced with control or SMARCE1 shRNAs. Gene expression is normalized to GAPDH and plotted as fold change relative to the control cell line ($n = 4$; mean ± SEM).

The larger of these modules encoded for multiple secreted proteases that degrade collagen and laminin, the two main components of basement membrane. Among these proteases were three collagen-degrading matrix metalloproteinases (MMPs): MMP1, MMP2, and MMP13 (11, 12). This module also included the urokinase plasminogen activator (*PLAU*) and its membranous receptor (*PLAUR*), which together degrade laminin (13). In addition, this module included ECM components that stimulate cancer cell invasion, such as *COL1A2*, fibronectin (*FN1*), periostin (*POSTN*), and SPARC, among others (see complete list of genes above). The module also included three lysyl oxidases (*LOX*, *LOXL1*, and *LOXL2*) that remodel ECM by cross-linking collagen, previously implicated in invasion (14). Given these observations, we refer to this set of genes as an "ECM invasion module."

To identify potential regulators of this ECM invasion module, we applied perturbation gene signatures and the Apriori algorithm to estimate the contributions of transcription and chromatin-modifying factors to module gene expression. This analysis identified SMARCE1 as a candidate regulator of the ECM invasion module ($P < 10^{-42}$; Fig. 1*B*); SMARCE1 was not identified as a candidate regulator of identically sized random gene modules (Fig. S1 *C* and *D*) (15). To validate that SMARCE1 regulates this module, we used shRNAs to inhibit SMARCE1 expression in the invasive SUM159 and MDA.MB.231 breast cancer cell lines (Fig. S2*A*). Whereas SMARCE1 inhibition significantly reduced the expression of genes in the ECM invasion module, it had no effect on the expression of a random set of control genes (Fig. 1*C* and Fig. S2*B*).

SMARCE1 Promotes Invasion Through Basement Membrane. We next assessed if SMARCE1 is required for cancer cells to up-regulate proteases and invade through basement membrane. When seeded into 3D basement membrane, the SUM159 and MDA.MB.231 breast cancer lines form clonal spheroids that are initially noninvasive but, over time, invade into the surrounding matrix (16, 17). One week after seeding, the cultured spheroids can be classified by automated image analyses as noninvasive (T-I), partially invasive (T-II) or highly invasive (T-III; Fig. 2*A* and Fig. S3 *A* and *B*). To quantify matrix protease activity, we supplemented the basement membrane cultures with a modified collagen (IV) substrate that fluoresces upon proteolytic cleavage. Although minimal in the noninvasive spheroids, MMP activity increased progressively upon invasion, with a fourfold increase in partially invasive spheroids and a 10-fold increase in highly invasive spheroids (Fig. S3*C*). Consistent with prior studies, this indicated that invasive progression is associated with up-regulated protease activity.

In the MDA.MB.231 and SUM159 lines, SMARCE1 inhibition almost completely blocked the formation of highly invasive spheroids (i.e., T-III) while also significantly reducing partially invasive spheroids (i.e., T-II; Fig. 2*B* and Fig. S3*D*); SMARCE1 inhibition had no effect on the number or size of the spheroids formed and overall cell numbers (Fig. 2*B* and Fig. S3 *D–F*). SMARCE1 inhibition also resulted in a 75% reduction in the activity of secreted matrix proteases that cleave collagen type IV (Fig. 2*B* and Fig. S3*D*). Consistent with these findings, SMARCE1 protein levels were elevated in partially and strongly invasive spheroids (Fig. S3*G*). To assess reversibility and sufficiency, we inhibited SMARCE1 expression with a doxycycline-inducible shRNA (Fig. S3*H*). Although doxycycline addition for 7 d led to a fivefold increase in noninvasive spheroids, reexpression of SMARCE1 by doxycycline removal was sufficient to trigger invasiveness within 30 h (Fig. 2 *C* and *D*). SMARCE1 overexpression also triggered invasiveness in the noninvasive HMLER breast cancer cell line (Fig. S3*I*). Collectively, these findings indicated that SMARCE1 was dispensable for proliferation, but was required for tumor spheroids to up-regulate protease activity and invade through basement membrane.

Because SMARCE1 is a component of the SWI/SNF complex, its inhibition could, in principle, disrupt the functions of the complex. If this were the case, disrupting the SWI/SNF complex would phenocopy SMARCE1 inhibition. However, inhibiting SMARCC1, a core component of the SWI/SNF complex, abolished cell growth (Fig. S4*A*). Because SMARCE1 is not required for proliferation (Fig. S4*B*), we conclude that its inhibition does not disrupt the core functions of the SWI/SNF complex.

SMARCE1 Is Required for Invasion and Metastasis in Vivo. We next assessed SMARCE1's in vivo function by using an orthotopic mouse model of human breast tumor formation and spontaneous metastasis. In this model, primary tumors are formed by introducing MDA.MB.231-LM2 cells stably expressing luciferase and GFP into the mammary glands of nonobese diabetic (NOD)/SCID mice. Inhibiting SMARCE1 had no effect on primary tumor growth (Fig. S5*A*); however, SMARCE1 inhibition significantly reduced local tumor invasion and entry into the circulation (Fig. 3 *A* and *B*). In contrast to control tumors, which had prominent invasive fronts with numerous cancers cells invading into the surrounding tissue, SMARCE1-inhibited tumors were well-encapsulated with few cells invading into the adjacent tissue (Fig. 3*A*). Mice harboring SMARCE1-inhibited tumors also exhibited 30-fold lower levels of circulating tumor cells (Fig. 3*B*).

In addition, inhibition of SMARCE1 resulted in a 500-fold reduction in lung metastases (Fig. 3*C*). Staining with an anti-GFP antibody further confirmed that the lungs of animals bearing SMARCE1-inhibited tumors were nearly devoid of cancer cells (Fig. S5*B*). To further clarify the steps in the metastatic cascade in which SMARCE1 was required, we performed tail-vein injections and longitudinally monitored lung metastasis. Eighteen days after injection, metastatic tumor burden was ~10-fold lower in mice injected with SMARCE1-inhibited cancer cells compared with mice injected with cells expressing a control LacZ shRNA (Fig. S5*C*). This 10-fold difference in metastatic

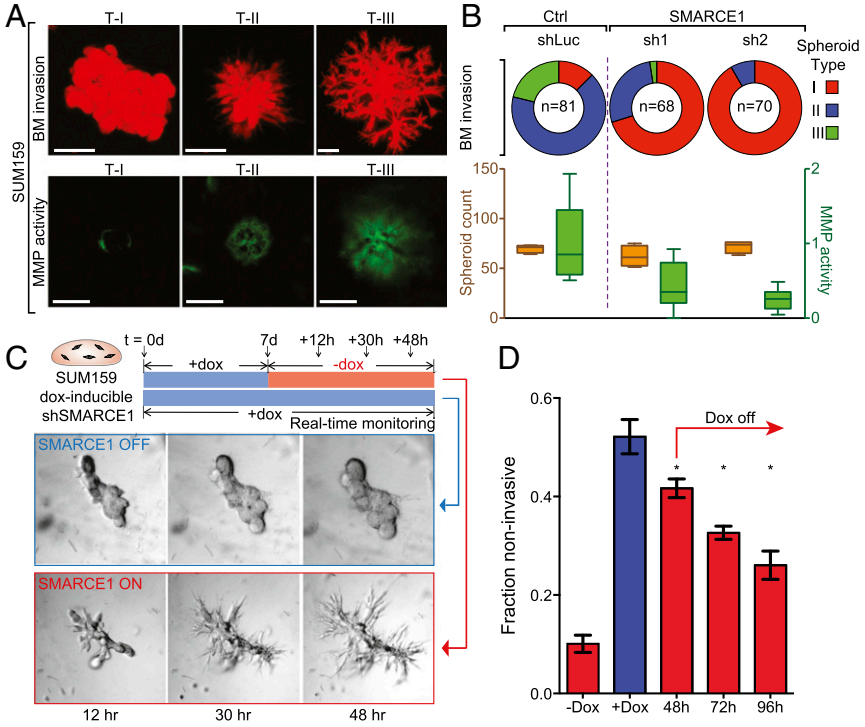

Fig. 2. SMARCE1 is required for cancer cell invasion through basement membrane. (*A*) Epifluorescence images of tumor spheroids formed by SUM159 cells in 3D basement membrane (BM). (*Top*) Noninvasive (T-I), partially invasive (T-II), or highly invasive (T-III) spheroids. (*Bottom*) Collagen IV hydrolysis (green) in DQ collagen IV-supplemented BM. (Scale bars: 100 μm.) (*B*) Quantification of tumor spheroid invasiveness, protease activity, and number in control and shSMARCE1 SUM159 cells. (*Top*) Quantification of T-I, T-II, and T-III spheroids. (*Bottom*) Spheroid MMP activity relative to shLuc controls and spheroid number per BM. (*C*) SMARCE1 reexpression rescues invasive progression in tumor spheroids. (*Top*) Experimental design to measure effect of SMARCE1 reexpression on spheroid invasiveness. (*Bottom*) Representative images of tumor spheroids 12, 30, and 48 h after doxorubicin (dox) withdrawal (SMARCE1 ON) or continued treatment with doxorubicin (SMARCE1 OFF). (*D*) Quantification of noninvasive spheroids after SMARCE1 inhibition for 7–9 d (+dox) and subsequent reexpression of SMARCE1 (dox off) for 48, 72, or 96 h. All spheroids were quantified at day 11 ($n = 4$; $^*P < 0.05$).

burden remained unchanged at later time points (Fig. S5*C*), suggesting that SMARCE1 was important specifically for extravasation or metastatic colony formation, but not for growth of the metastases within the lung parenchyma. Collectively, these observations indicated that SMARCE1 is required for the invasion and metastasis of breast cancers, but is dispensable for their growth.

SMARCE1 Predicts Prognosis in Patients with Early-Stage Tumors. We next investigated the clinical relevance of these findings by assessing if SMARCE1 expression could be used to prospectively identify breast tumors with a propensity to metastasize. Immunostaining for SMARCE1 in tissue microarrays indicated that its expression was lowest in early-stage breast cancers, increased during tumor progression, and was highest in tumors invading into adjacent lymph nodes ($P = 0.007$; Fig. 4*A*). Patients with early-stage breast tumors expressing high levels of SMARCE1 were significantly more likely to show relapse with metastases over a follow-up period of more than 15 y [hazard ratio (HR) = 4.13, $P < 0.0003$; Fig. 4*B*]. Importantly, this prognostic value was observed across multiple independent breast cancer datasets (Fig. S6*A*) and was independent of confounding factors such as grade and tumor size (Fig. S6 *B* and *C*). In contrast, SMARCE1 expression was not predictive of metastasis for patients diagnosed with later-stage tumors that had already invaded to adjacent lymph nodes (Fig. 4*C* and Fig. S6*D*). In addition, stratifying tumors based on expression of other members of the SWI/SNF complex was not predictive of metastasis (Fig. S6 *E*–*H*).

Stratifying by SMARCE1 expression had similar prognostic value for other types of epithelial tumors. In patients diagnosed with early-stage lung cancers, SMARCE1 expression was strongly predictive of future relapse and metastasis (HR = 7.30, $P < 0.0001$; Fig. S6*I*), but was not predictive for patients diagnosed with later-stage lung cancers (Fig. S6*J*). SMARCE1 expression was also predictive of relapse in early-stage ovarian cancers (HR = 3.35, $P = 0.0052$; Fig. S6*K*), but had no predictive value for later-stage cancers (Fig. S6*L*). These findings complemented the functional observations detailed earlier and indicated that SMARCE1 expression is strongly predictive of relapse and metastasis for early-stage tumors.

SMARCE1 Is Required to Escape the Ductal-Lobular Architecture of Normal Mammary Tissues. Breast tumors are initially confined in situ within the architecture of normal mammary tissue. To assess SMARCE1 in this context, we used a recently reported 3D model that supports the outgrowth of mammary tissues from

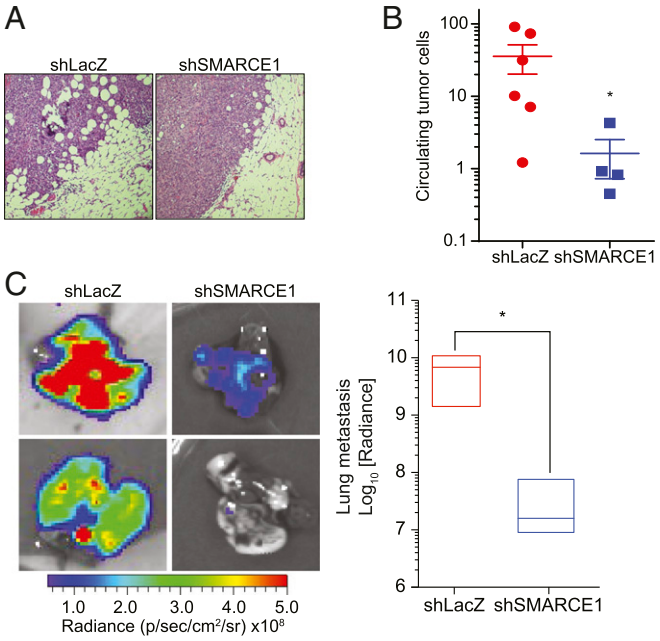

Fig. 3. SMARCE1 is essential for metastasis in vivo. (*A*) Representative H&E-stained sections of the tumor boundary from MDA.MB.231-LM2–injected control (shLacZ) and SMARCE1-inhibited (shSMARCE1) tumors 4 wk after injection. (*B*) Number of circulating tumor cells in mice bearing control ($n = 6$) or SMARCE1-inhibited ($n = 4$) tumors. (*C*) Representative luminescence images and quantification of metastatic burden in whole lungs of mice inoculated with shLacZ ($n = 3$) or shSMARCE1 ($n = 4$) MDA.MB.231-LM2 cells ($^*P < 0.05$).

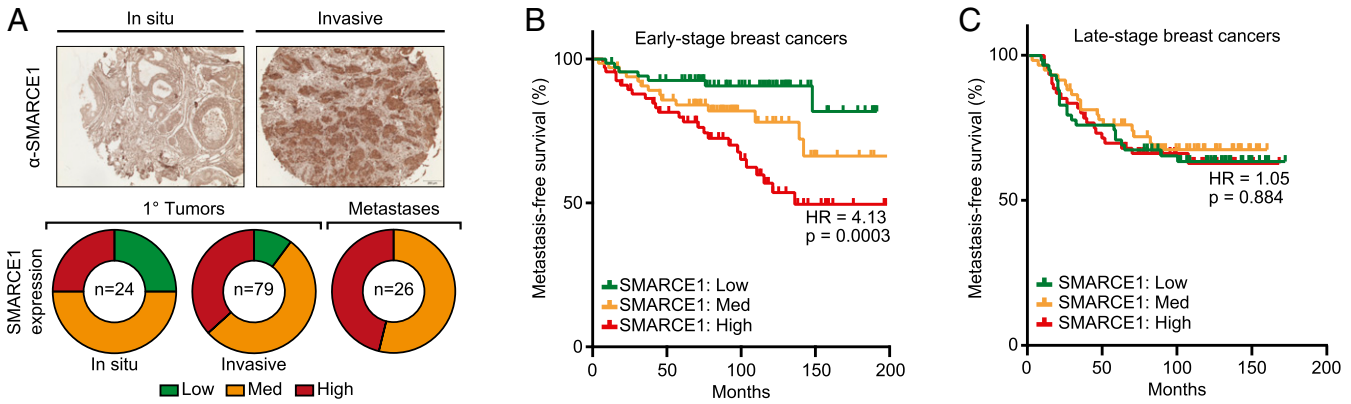

Fig. 4. SMARCE1 expression is prognostic in early-stage tumors. (*A*) Patient breast tissues from in situ and invasive breast cancers were immunohistochemically stained for SMARCE1 (*Top*). In situ breast cancer, invasive breast cancer, and metastasis staining intensities were quantified (*Bottom*). (*B* and *C*) SMARCE1 expression was examined in a cohort of patients with early-stage breast tumors [N stage 0 (lymph node-negative), GSE11121; $n = 200$] and late-stage breast tumors (N stage ≥ 1, GSE20685; $n = 190$). Metastasis-free survival curves in patients stratified into tertiles (high, medium, low) based on tumor SMARCE1 expression. HRs and *P* values were determined with the log-rank statistical test.

primary human breast cells (18). In this model, human mammary tissues are expanded in hydrogels that mimic the microenvironment of the human breast (Fig. S7*A*) (18). To model in situ cancer, we microinjected fluorescently labeled cancer cells into the expanded mammary tissues (Fig. 5*A*).

When inoculated in situ, SUM159-dsRed breast cancer cells proliferated and, over a span of 6 d, migrated to ducts and lobules adjacent to the initial site of injection. As early as 3 d after inoculation, the cells projected long filopodia (>100-μm average length) into the surrounding matrix (Fig. 5 *B*–*F*). By 11 d, a subset of the inoculated cancer cells had escaped into the surrounding ECM (Fig. 5*B* and Fig. S7*B*). In contrast, nonneoplastic MCF10A cells only spread internally within the mammary tissues and were unable to invade into the surrounding ECM (Fig. 5*B* and Fig. S7*B*).

When SMARCE1 expression was inhibited, the SUM159 cells still proliferated and spread to adjacent ducts and lobules within the normal breast tissues, indicating that SMARCE1 was dispensable for both of these processes. However, the SMARCE1-inhibited cells were unable to extend filopodial projections or invade into the surrounding ECM (Fig. 5 *B*–*F*). To control for differences in proliferation, we coinjected dsRed-labeled SUM159 cells expressing a control shRNA together with Venus-labeled SUM159 cells inhibited for SMARCE1 expression into shared tissues. The proliferation rates of these lines were indistinguishable, indicating that differences in proliferation were not responsible for the phenotypic differences observed (Fig. S7*C*).

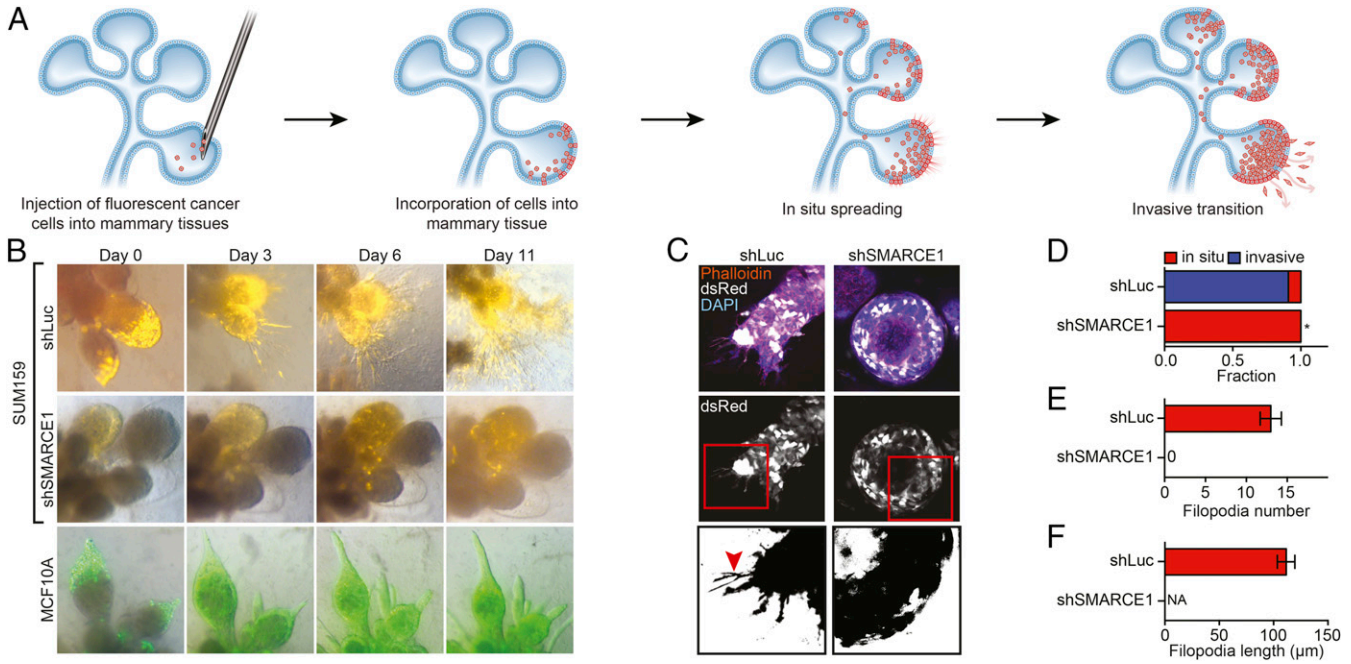

Fig. 5. SMARCE1 is required for cancers to escape the ductal-lobular architecture of normal mammary tissues. (*A*) Schematic of the tissue model of invasive progression of in situ cancer cells. (*B*) Representative bright-field images with a fluorescent overlay of dsRed-labeled SUM159 cells transduced with shLuc or shSMARCE1 (pseudocolored yellow) and Venus-labeled MCF10A cells injected into mammary tissues. (*C*) Confocal images of tissues 3 d postinjection. Red arrowhead indicates filopodia. (*D*) Fraction of SUM159 cells (shLuc or shSMARCE1) that remained encapsulated (in situ) or escaped the tissue architecture (invasive) 3 d postinjection. (*E*) Number of filopodia formed by SUM159 cells per tissue injected in *D*. (*F*) Length of the filopodia from *E* (*$P < 0.05$).

These observations indicated that SMARCE1 was dispensable for proliferation and migration of cancer cells growing in situ, but was essential for their escape from the normal tissue architecture and invasion into the surrounding matrix.

SMARCE1 Binds ILF3 and Is Recruited to ILF Motifs. To probe SMARCE1's function, we identified its binding partners in noninvasive and invasive cells by using immunoprecipitation (IP)-MS (Fig. S8*A*). To determine if SMARCE1 binds to its partners together with the SWI/SNF complex, we also performed IP-MS against a core component of the complex (SMARCC1). As expected, SMARCE1 and SMARCC1 were both associated with the SWI/SNF complex in the invasive and noninvasive cells (Fig. 6*A*). However, SMARCE1 was uniquely bound to one factor, ILF3, specifically in invasive cells. Unlike SMARCE1, SMARCC1 did not bind ILF3 in noninvasive or invasive cells. These findings indicated that SMARCE1 specifically interacts with ILF3 in invasive cells independently of the core SWI/SNF complex (Fig. 6 *A* and *B*).

Because SMARCE1 lacks a sequence-specific DNA binding domain, these findings suggested a model in which ILF3 could be directing the genomic localization of SMARCE1. If this were the case, we would expect ILF3 to also be required for the expression of SMARCE1-regulated genes, in particular those in the ECM-invasion module. Consistent with this, mouse embryonic fibroblasts overexpressing ILF3 up-regulated nearly all of the genes in the SMARCE1-regulated ECM invasion module (63 of 81; $P < 7.1 \times 10^{-8}$; Fig. 6*C*) (19). Moreover, inhibition of ILF3 caused a twofold reduction in the formation of invasive spheroids in the 3D basement membranes (Fig. 6*D*). However, unlike SMARCE1, ILF3 expression was not correlated with or predictive of progression in patients with early-stage cancers ($P = 0.0685$; Fig. S8*B*), suggesting that its mRNA expression is not limiting in patient tumors.

We next performed ChIP and sequencing (ChIP-seq) to identify the binding sites of SMARCE1 in the genomes of noninvasive and invasive cells (Fig. 6*E*) and examine their proximity to ILF3 motifs. SMARCE1 was bound to ~550 genomic sites in noninvasive cells, and 58% of these sites were also bound by SMARCE1 in invasive cells (321 of 554; $P < 0.01$; Fig. S8*C*). However, SMARCE1 was bound to an additional 8,000 sites in invasive cells (Fig. S8*C*), the majority of which were localized to regulatory regions with acetylated H3K27 histones (63% in invasive vs. 7% in noninvasive; $P < 0.01$). The SMARCE1-bound sites in invasive cells were strongly enriched at the enhancers of genes associated with DCIS progression ($P < 0.01$; see Fig. 1). In addition, the SMARCE1-bound sites in invasive cells were frequently associated with ILF3 motifs, which, when present, were invariably found at the center of the SMARCE1-bound sites (Fig. 6*F*). In contrast, ILF3 motifs were not enriched at SMARCE1-bound sites in noninvasive cells or at SMARCC1 binding sites (Fig. 6*F* and Fig. S8*D*). These findings were consistent with the observation that SMARCE1 binds to ILF3 only in invasive cells, and further supported a model in which ILF3 was directing the genomic localization of SMARCE1 in invasive cells.

Discussion

These observations establish SMARCE1 as a clinically relevant driver of the invasive progression of early-stage breast cancers. We find that SMARCE1 drives invasion by regulating a module of genes encoding proinvasive ECM and secreted proteases that degrade basement membrane. In functional studies in 3D cultures and animal models, SMARCE1 is dispensable for tumor growth but is required for the invasive and metastatic progression of cancers. The clinical relevance of these findings is underscored by how we were first led to SMARCE1—namely through the analysis of heterogeneous breast tumors containing regions of DCIS and invasive cancer—and by our subsequent analyses of hundreds of patient tumors, indicating that its expression is strongly predictive of metastasis across a spectrum of cancer types.

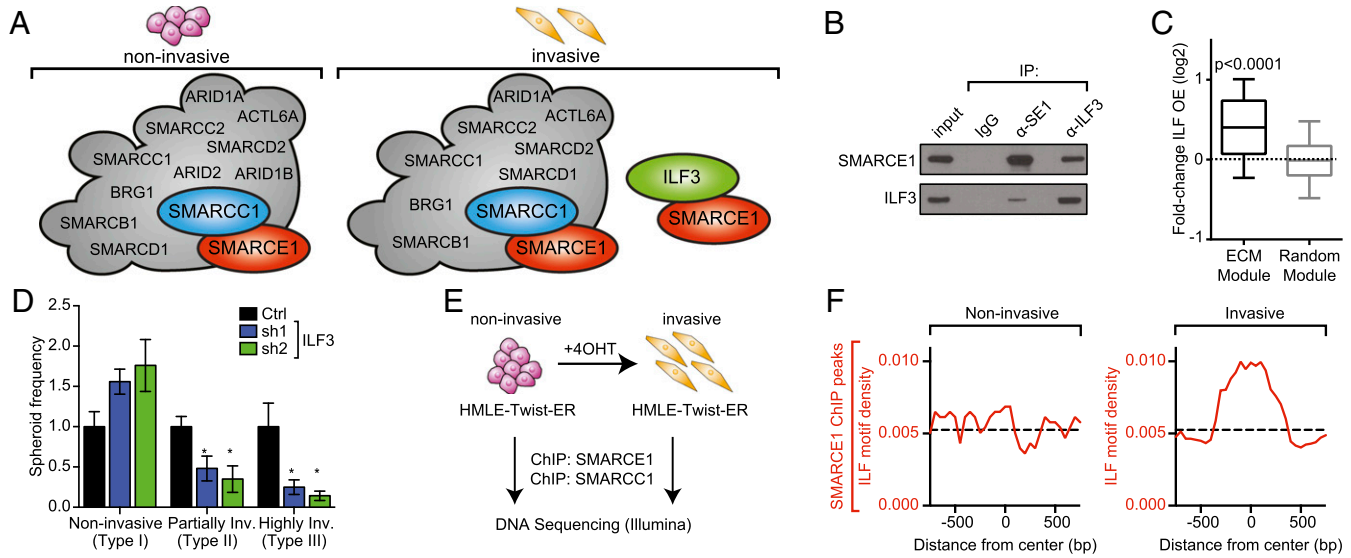

Fig. 6. SMARCE1 binds ILF3 and is recruited to ILF motifs. (*A*) Schematic representation of the list of binding partners of SMARCE1 or SMARCC1 in noninvasive or invasive HMLE-Twist-ER cell [untreated or treated with 125 nM 4-hydroxytamoxifen (4OHT), respectively] identified by co-IP and MS. SMARCE1 and SMARCC1 interacted with each other as well as other members of the SWI/SNF complex (shown in gray) in invasive and noninvasive cells. An additional unique interaction between SMARCE1 and ILF3 was detected in invasive HMLE-Twist-ER cells. (*B*) Co-IP of endogenous SMARCE1 (SE1) and ILF3 in nuclear lysates from invasive SUM159 cells. (*C*) Expression of the ECM invasion module or a random module of 88 genes in embryonic fibroblasts from transgenic mice overexpressing ILF2/3 (GSE67591) relative to expression in genetically matched mice without ILF2/3 overexpression. (*D*) Quantification of tumor spheroid invasiveness in control (shLuc) or shILF3 (sh1, sh2) SUM159 cells grown in basement membrane. (*E*) Experimental design for ChIP and sequencing (ChIP-seq) of SMARCC1 and SMARCE1 in noninvasive and invasive HMLE-Twist-ER cells (untreated or treated with 125 nM 4OHT, respectively). (*F*) SMARCE1 is localized to ILF motifs specifically in invasive HMLE-Twist-ER cells. Motif density was calculated by using a sliding window of 50 bp extending to 750 bp on either side of SMARCE1-bound peaks identified by ChIP-seq (*$P < 0.05$).

Currently, most women with early-stage tumors are treated with breast-conserving surgery (i.e., lumpectomy) followed by localized radiation. Although effective for most early-stage tumors, this treatment leads to recurrence with metastasis in ~25% of women with lymph node-negative stage I or stage IIA cancers over a follow-up period of 10 y (20). Our analyses of patient tumors indicate that these poor-prognosis cancers express high levels of SMARCE1 at the time of diagnosis. As a consequence, stratifying patients on the basis of SMARCE1 expression would prospectively identify a subset of early-stage tumors that would be better treated with a more aggressive therapy regimen.

Conversely, epidemiological studies have suggested that more than half of DCIS lesions are indolent and would never become life-threatening if left untreated (7, 21). This has led to an increasing awareness that the current clinical paradigm may be overtreating a significant fraction of women diagnosed with indolent DCIS tumors. To rigorously assess this possibility, several clinical trials are currently under way to determine whether watchful surveillance would lead to equivalent outcomes for such women. Our findings indicate that SMARCE1 should be added to the pathological features used to identify indolent DCIS lesions that are candidates for watchful surveillance.

Although our functional studies focused exclusively on SMARCE1's role in breast cancer, our analyses of the expression profiles of patient tumors suggest that it is likely to also play an important role in regulating the invasiveness of other cancer types. High SMARCE1 expression is predictive of relapse and prognosis in early-stage lung and ovarian cancers, but provided little predictive value for later-stage cancers of these types. This suggests that these tumors use a common underlying mechanism to invade and, ultimately, metastasize. Consistent with this, a shared functional requirement for the invasive progression of all carcinomas is the degradation of the basement membrane that surrounds epithelial tissues. This is the very function conferred by SMARCE1 through the up-regulation of proteases that degrade collagen IV and laminins.

At a mechanistic level, prior studies of SMARCE1 function have focused on its ability to recruit the SWI/SNF complex to genes regulated by hormone receptors (22–24). However, our ChIP-seq and MS observations indicate that SMARCE1 binds most enhancers in the absence of hormone receptors and the SWI/SNF complex, indicating that both are dispensable for SMARCE1's regulatory functions in invasive cells. Moreover, our findings suggest that ILF3 is a key cofactor that mediates SMARCE1's proinvasive regulatory functions. Further study will be needed to determine how SMARCE1 partitions between ILF3-bound and SWI/SNF-bound complexes, and why our findings contrast with those of a recently published study on SMARCE1 in breast cancer (25).

To date, experimental studies of early-stage breast cancer have been significantly limited by a lack of model systems that faithfully recapitulate the tissue microenvironment of early-stage lesions as they occur in human breast tissue. We have addressed this limitation by contributing a model of breast cancer progression in which human cancer cells are integrated in situ into the ductal-lobular architecture of primary human mammary tissues. The development of this model leverages a recently reported method for expanding primary human mammary tissues in culture by using 3D hydrogel scaffolds (18). Because comparable methods have recently been reported for other human tissue types (26, 27), we are hopeful that the strategy used here will prove broadly useful for modeling in situ tumors arising within the relevant human tissue microenvironment.

Materials and Methods

In vivo and 3D hydrogel studies were performed as previously described (18, 28). All computational analyses, reagents, public datasets used, and other protocols are described in *SI Materials and Methods*.

ACKNOWLEDGMENTS. We thank Wendy Salmon for assistance with microscopy and Prof. Hazel Sive for sharing microinjection equipment. This research was supported by National Science Foundation Graduate Research Fellowship Grant 1122374 (to E.S.S.), a Ludwig Fund for Cancer Research fellowship (to Y.-X.F), and a grant from the Ludwig Fund for Cancer Research.

1. Place AE, Jin Huh S, Polyak K (2011) The microenvironment in breast cancer progression: Biology and implications for treatment. *Breast Cancer Res* 13:227.
2. Howlader N, et al. (2016) *SEER Cancer Statistics Review, 1975-2013* (National Cancer Institute, Bethesda, MD).
3. Kerlikowske K, et al. (2010) Biomarker expression and risk of subsequent tumors after initial ductal carcinoma in situ diagnosis. *J Natl Cancer Inst* 102:627–637.
4. Schuetz CS, et al. (2006) Progression-specific genes identified by expression profiling of matched ductal carcinomas in situ and invasive breast tumors, combining laser capture microdissection and oligonucleotide microarray analysis. *Cancer Res* 66:5278–5286.
5. Hernandez L, et al. (2012) Genomic and mutational profiling of ductal carcinomas in situ and matched adjacent invasive breast cancers reveals intra-tumour genetic heterogeneity and clonal selection. *J Pathol* 227:42–52.
6. Yao J, et al. (2006) Combined cDNA array comparative genomic hybridization and serial analysis of gene expression analysis of breast tumor progression. *Cancer Res* 66:4065–4078.
7. Sanders ME, Schuyler PA, Dupont WD, Page DL (2005) The natural history of low-grade ductal carcinoma in situ of the breast in women treated by biopsy only revealed over 30 years of long-term follow-up. *Cancer* 103:2481–2484.
8. Collins LC, et al. (2005) Outcome of patients with ductal carcinoma in situ untreated after diagnostic biopsy: Results from the Nurses' Health Study. *Cancer* 103:1778–1784.
9. Bleyer A, Welch HG (2012) Effect of three decades of screening mammography on breast-cancer incidence. *N Engl J Med* 367:1998–2005.
10. Wang X, Dalkic E, Wu M, Chan C (2008) Gene module level analysis: Identification to networks and dynamics. *Curr Opin Biotechnol* 19:482–491.
11. Knäuper V, López-Otin C, Smith B, Knight G, Murphy G (1996) Biochemical characterization of human collagenase-3. *J Biol Chem* 271:1544–1550.
12. Matrisian LM (1990) Metalloproteinases and their inhibitors in matrix remodeling. *Trends Genet* 6:121–125.
13. Nakagami Y, Abe K, Nishiyama N, Matsuki N (2000) Laminin degradation by plasmin regulates long-term potentiation. *J Neurosci* 20:2003–2010.
14. Siegel RC, Fu JC, Chang Y (1976) Collagen cross-linking: The substrate specificity of lysyl oxidase. *J Biol Chem* 251(18):5779–5785.
15. Wilson BG, Roberts CWM (2011) SWI/SNF nucleosome remodellers and cancer. *Nat Rev Cancer* 11:481–492.
16. Petersen OW, Rønnov-Jessen L, Howlett AR, Bissell MJ (1992) Interaction with basement membrane serves to rapidly distinguish growth and differentiation pattern of normal and malignant human breast epithelial cells. *Proc Natl Acad Sci USA* 89: 9064–9068.
17. Weaver V, Petersen O (1997) Reversion of the malignant phenotype of human breast cells in three-dimensional culture and in vivo by integrin blocking antibodies. *J Cell Biol* 137(1):231–245.
18. Sokol ES, et al. (2016) Growth of human breast tissues from patient cells in 3D hydrogel scaffolds. *Breast Cancer Res* 18:19.
19. Todaka H, et al. (2015) Overexpression of NF90-NF45 represses myogenic MicroRNA biogenesis, resulting in development of skeletal muscle atrophy and centronuclear muscle fibers. *Mol Cell Biol* 35:2295–2308.
20. Schmidt M, et al. (2008) The humoral immune system has a key prognostic impact in node-negative breast cancer. *Cancer Res* 68:5405–5413.
21. Alvarado M, Ozanne E, Esserman L (2012) Overdiagnosis and overtreatment of breast cancer. *Am Soc Clin Oncol Educ Book* e40–e45.
22. Link KA, et al. (2005) BAF57 governs androgen receptor action and androgen-dependent proliferation through SWI/SNF. *Mol Cell Biol* 25:2200–2215.
23. García-Pedrero JM, Kiskinis E, Parker MG, Belandia B (2006) The SWI/SNF chromatin remodeling subunit BAF57 is a critical regulator of estrogen receptor function in breast cancer cells. *J Biol Chem* 281:22656–22664.
24. Balasubramaniam S, et al. (2013) Aberrant BAF57 signaling facilitates prometastatic phenotypes. *Clin Cancer Res* 19:2657–2667.
25. Sethuraman A, et al. (2016) SMARCE1 regulates metastatic potential of breast cancer cells through the HIF1A/PTK2 pathway. *Breast Cancer Res* 18:81.
26. Dye BR, et al. (2015) In vitro generation of human pluripotent stem cell derived lung organoids. *eLife* 4:e05098.
27. Sato T, et al. (2011) Long-term expansion of epithelial organoids from human colon, adenoma, adenocarcinoma, and Barrett's epithelium. *Gastroenterology* 141: 1762–1772.
28. Feng Y, et al. (2014) Epithelial-to-mesenchymal transition activates PERK-eIF2a and sensitizes cells to endoplasmic reticulum stress. *Cancer Discov* 4(6):702–715.
29. Minn AJ, et al. (2005) Genes that mediate breast cancer metastasis to lung. *Nature* 436:518–524.
30. Gyorffy B, Lánczky A, Szállási Z (2012) Implementing an online tool for genome-wide validation of survival-associated biomarkers in ovarian-cancer using microarray data from 1287 patients. *Endocr Relat Cancer* 19:197–208.
31. Marson A, et al. (2008) Connecting microRNA genes to the core transcriptional regulatory circuitry of embryonic stem cells. *Cell* 134(3):521–533.